ACOUSTICS 2017 PERTH
SOUND, SCIENCE AND SOCIETY

Target Tracking Using Seabed Based Passive Acoustic Arrays

Jimmy Wang, Sanjeev Arulampalam, Fiona Fletcher, Matthew Steed and Vincent Rose

Maritime Division, DST Group, Edinburgh, SA 5111, Australia

ABSTRACT

Passive sonar systems are a key sensor type for anti-submarine warfare, used to detect acoustic energy emitted by surface or subsurface sources. These systems typically provide bearing detections from targets that are loud enough to be detected. Over time, these bearing detections can be associated and fused to generate a track on a target, provided observability criteria are met (usually by manoeuvring the sensor, or having multiple sensors in contact with the target).

In this paper, we consider an experimental passive acoustic seabed array sensor system consisting of three line arrays of hydrophones deployed on the sea floor. We use detections from this system to explore the challenges involved with tracking targets using passive seabed array systems. A tracker has been developed using the Cubature Kalman filter for estimation with global nearest neighbour data association. This tracker has been applied to two datasets collected using the experimental seabed array system.

1 INTRODUCTION

Passive sonar systems are a key sensor type for anti-submarine warfare, used to detect acoustic energy emitted by surface or subsurface sources. Passive sonar systems can be fitted to submarines and surface ships or deployed and operated remotely, such as sonobuoys or seabed array systems. The goal of such systems is to detect, localise, classify and track any surface or sub-surface contacts.

In this paper, we consider an experimental passive acoustic seabed array sensor system consisting of three line arrays of hydrophones that are deployed on the sea floor. The system generates bearing detections from each array for targets that are sufficiently loud to be detected. The aim of this work is to explore the challenges associated with tracking targets using this system, with the ultimate goal of developing a robust automated tracking system. In this paper, we present the results of the application to sea trial data of a tracking algorithm developed using Cubature Kalman filter estimation and global nearest neighbour data association.

Section 2 gives a brief description of the seabed arrays, the trial itself and data collected on the trial. Two data sets collected during the sea trial were used to test the tracking algorithms. Section 3 describes the state estimation and data association algorithms employed in this study. Track management, including track initiation, confirmation and termination, is also discussed in this section. Section 4 presents the tracking results and conclusions are given in Section 5.

2 SEABEAD ARRAY, SEA TRIAL AND SEA TRIAL DATA

Maritime Division of DST Group has developed an experimental acoustic seabed array system. It consists of a set of line arrays of equally spaced hydrophones that are deployed on the sea floor. This system can be utilised for the passive surveillance of a large area for both surface and subsurface targets.

A sea trial was conducted with three seabed arrays deployed. Two datasets were recorded during this trial with targets of opportunity detected using all three arrays laid on the sea floor. The array separation, estimated array shapes and array orientations are shown in Figure 1. Figure 2 shows the trial scenarios for which Dataset A (left) and Dataset B (right) were collected. Dataset A had duration of 90 minutes with a merchant ship, Target A, detected. Target A travelled north easterly and made a turn of 360 degrees, producing a loop in its trajectory. Dataset B has duration of approximately 130 minutes with two merchant ships detected. Target B travelled south westerly, while Target C travelled north easterly (Figure 2).

A Bearing Time Record (BTR) is a commonly used sonar display, in which the *x*-axis represents directions (bearings), the *y*-axis represents time and the colour represents the intensity of the signal. Each row of the BTR displays the values of signal strength at that time for all directions. Bearings are measured clockwise from True North. Figure 3 shows the BTRs for Arrays 1 and 2 for Dataset A. The bearing track of Target A is clearly shown as the dark red lines in each of the BTRs. If a target is detected by a perfect line array, then a pair of symmetric

bearing tracks about the orientation of the array will appear in the BTR. This is called Left and Right ambiguity. Basically, one cannot tell whether the target is on the left or right side of the array. Observe that the bearing tracks in each of the BTRs are not perfectly symmetric, one is stronger than the other. This is because, in practice, the arrays are not perfectly straight when deployed on the sea floor as shown in the array shapes depicted in Figure 1.

As shown in Figure 1, the orientations of Arrays 2 and 3 have only a small difference. As a consequence, BTRs and bearing detections plots from these two arrays are quite similar. For this reason, future discussions will be restricted to bearing data collected by Arrays 1 and 2.

The detection algorithm used for the sea trial data is based on finding a peak compared to neighbouring beams. The target actual bearings in relation to the arrays are calculated from the GPS recording of the merchant ships. The bearing detections and the actual bearings for Dataset A are displayed in Figure 4.

The BTRs for Dataset B are depicted in Figure 5 and show the merchant ship bearing tracks clearly. As described above, because the seabed array is a line array, the BTR also contains the ambiguous bearing track of the targets. Figure 6 shows the bearing detections and actual bearings of Target B and Target C.

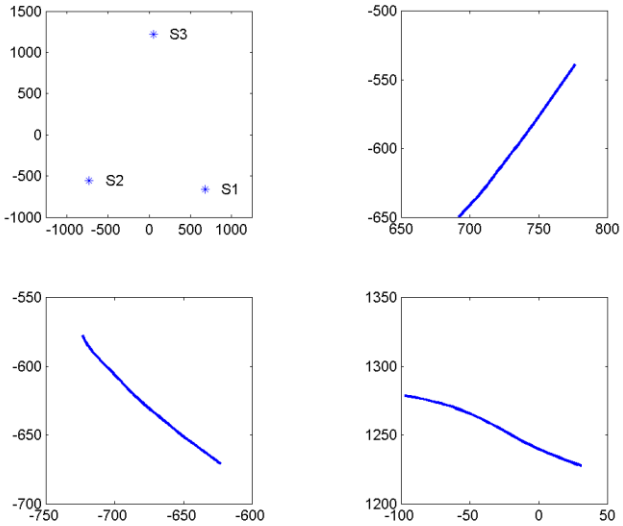

Figure 1 Array centre locations (in metres) with respect to the origin (top left) and shape of Array 1 (top right), Array 2 (bottom left) and Array 3 (bottom right).

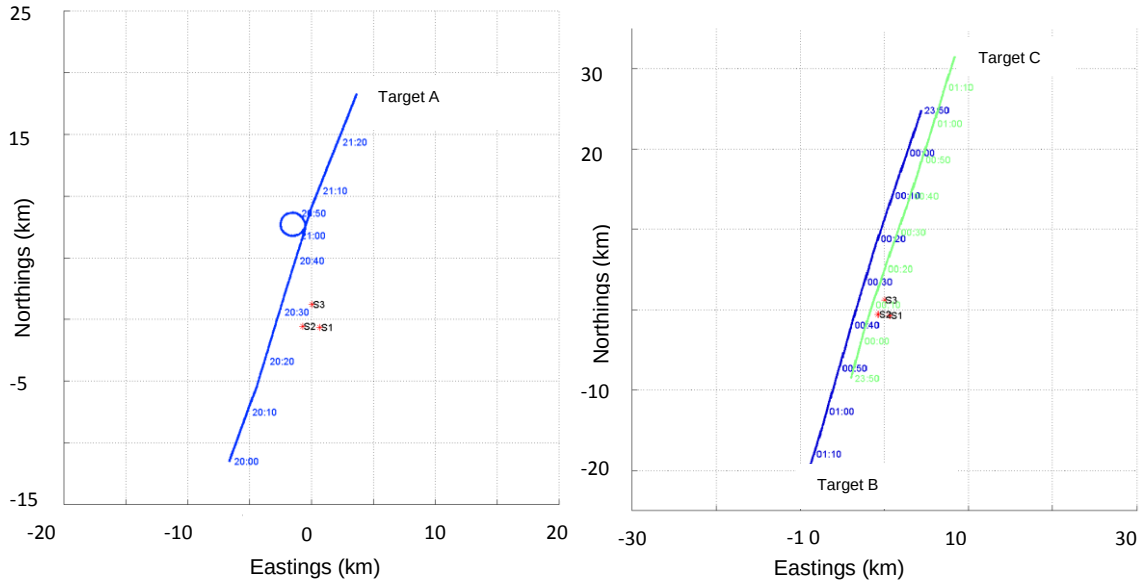

Figure 2 Target and array scenarios for Dataset A (left) and Dataset B (right)

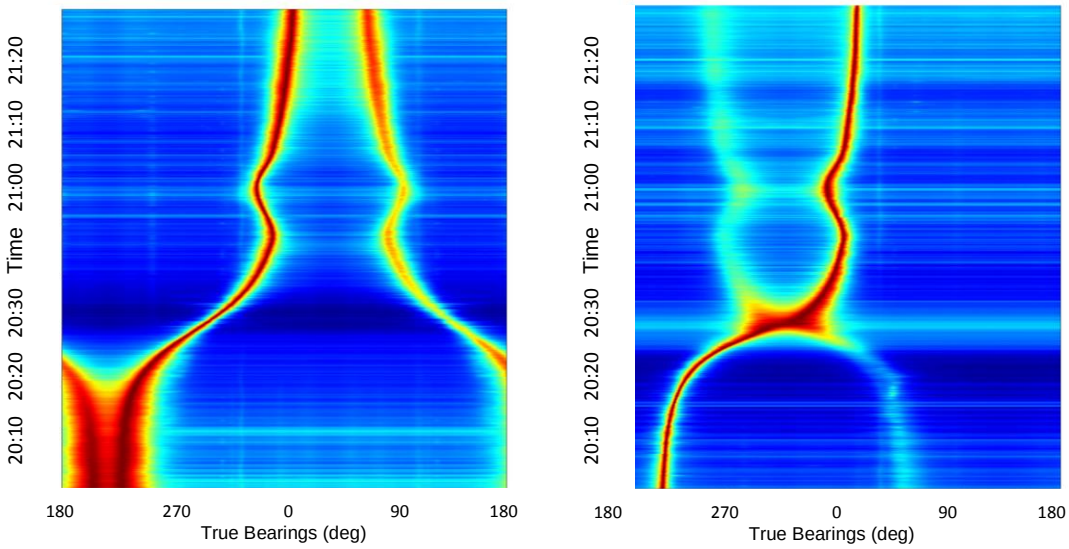

Figure 3 Bearing Time Record (BTR) displays for Arrays 1 and 2 for Dataset A

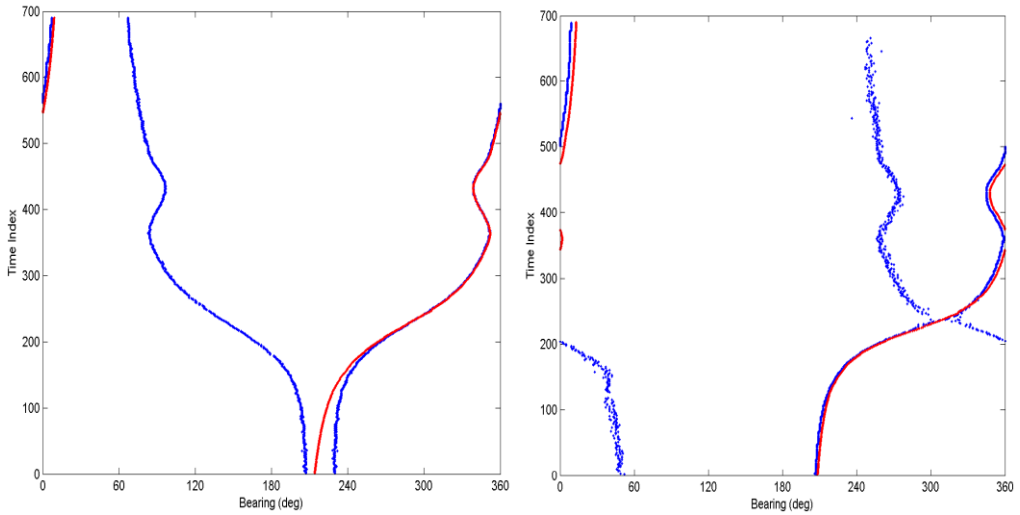

Figure 4 Bearing detections in blue and actual bearings in red of Array 1 (left) and Array 2 (right) for Dataset A

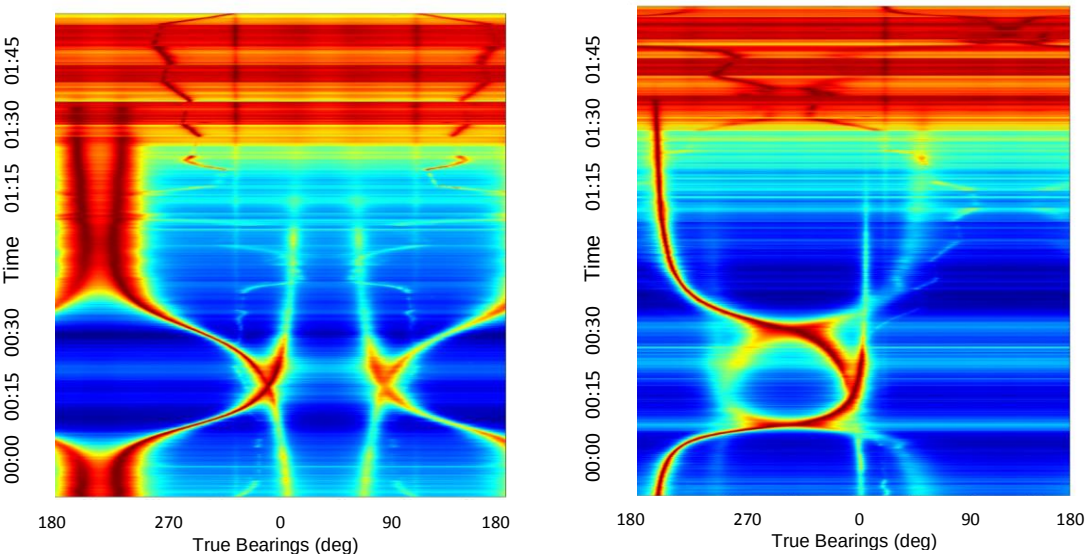

Figure 5 Bearing Time Record (BTR) displays for Arrays 1 and 2 for Dataset B

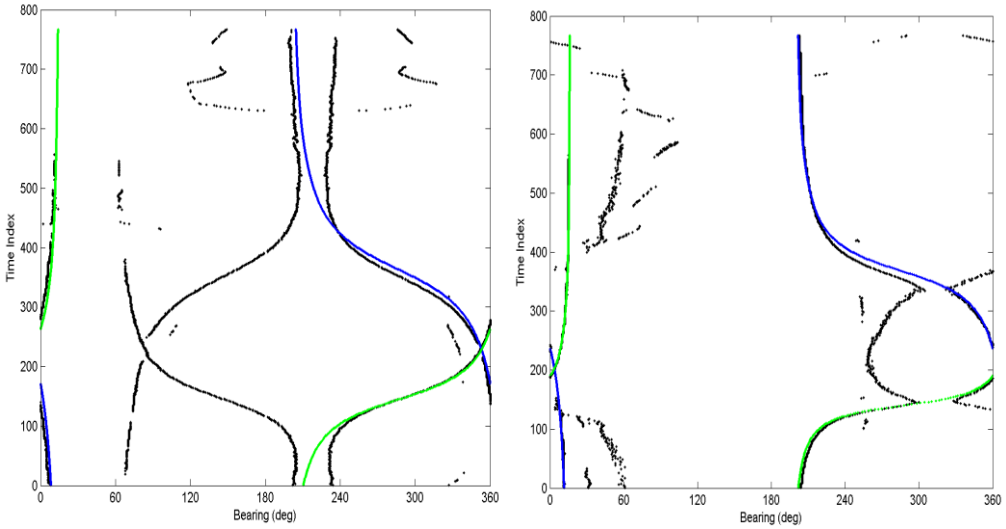

Figure 6 Bearing detections in black and actual bearings in blue and green of Array 1 (left) and Array 2 (right) for Dataset B

From Figure 4, it is easy to see that the error between the actual and detected bearings exhibit a strong bias, especially at the beginning for Array 1. Figure 7 shows the error between the actual bearings and the detected bearings for arrays 1 and 2 for Dataset A. The almost 16 degrees error at the beginning for Array 1 is likely to cause significant track initialisation error. The large bearing error is mostly caused by the fact that the target was located near the endfire direction of the array. The bias is also likely to result in output state-estimation errors.

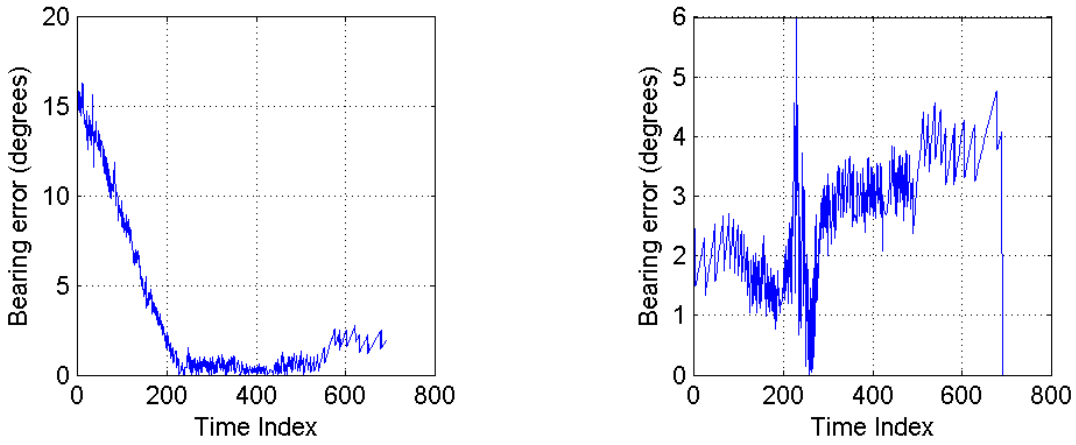

Figure 7 Bearing measurement bias of Array 1 (left) and Array 2 (right) for Target A in Dataset A

3 STATE ESTIMATION, DATA ASSOCIATION AND TRACK MANAGEMENT

The purpose of a state estimation algorithm is to estimate the target state, which may include position, velocity and other parameters, using a set of associated noise-corrupted measurements over time. A number of state estimation algorithms have been developed (Bar-Shalom and Fortmann 1988, Blackman and Popoli 1999, Ristic, Arulampalam and Gordon 2004). In this study, a more recently developed recursive parameter estimation algorithm known as the *Cubature Kalman Filter* (CKF) (Arasaratnam 2009, Arasaratnam and Haykin 2009, Arasaratnam, Haykin and Hurd 2010) is chosen. For the passive sonar target tracking problem with bearings-only measurements, the state transition and the measurement equations are

$$\begin{aligned} \mathbf{x}(k+1) &= F(k)\mathbf{x}(k) + \mathbf{u}(k) \\ \mathbf{z}(k) &= h(\mathbf{x}(k)) + \mathbf{v}(k) \end{aligned} \tag{1}$$

where $\mathbf{x}(k)$ is the state vector of *x, y* position and *x, y* velocity at time instant k, $F(k)$ is the known state transition matrix, $\mathbf{z}(k)$ is the bearing measurement, $\mathbf{u}(k)$ and $\mathbf{v}(k)$ are zero mean Gaussian noise vectors with known covariances. The non-linear bearings are calculated according to

$$h(\mathbf{x}(k)) = \arctan[(x(k) - xa)/(y(k) - ya)],$$

where $[x(k), y(k)]$ is the estimated target location at time k and $[xa, ya]$ is the centre location of the array whose detection is used for the track update. This measurement equation involves a nonlinear arctangent function. Therefore, the Kalman filter cannot be directly applied to these measurements because the multidimensional integral for the posterior density, i.e., the conditional probability density given the measurements, has no closed form solution. However, the CKF is an algorithm that numerically approximates this integral using the cubature-point sets $\{\omega_i, \xi_i\}$ defined below. Let σ_θ be the standard deviation of $\mathbf{v}(k)$, $n_x = 4$ be the length of the state vector, $\omega_i = 1/(2n_x), i = 1, 2, ..., 2n_x$ and

$$\Xi = \sqrt{n_x}[A \quad B]$$

be a 4x8 matrix with A being the 4x4 identity matrix and $B = -A$. ξ_i is the i-th column of the Ξ matrix. Then the transformed points which are used to approximate the integral are calculated as

$$\alpha(i, k+1|k) = \sqrt{P(k+1|k)}\,\xi_i + \hat{\mathbf{x}}(k+1|k), \qquad i = 1, 2, ..., 2n_x.$$

The predicted bearing measurement

$$\hat{\mathbf{z}}(k+1|k) = \sum_{i=1}^{2n_x} \omega_i\, \beta(i, k+1|k), \quad \text{where} \quad \beta(i, k+1, k) = h[\alpha(i, k+1|k)].$$

The Kalman gain can then be calculated according to

$$W(k+1) = P_{xz}(k+1|k) S^{-1}(k+1|k),$$

where the cross-covariance is

$$P_{xz}(k+1|k) = \sum_{i=1}^{2n_x} \omega_i [\alpha(i, k+1|k) - \hat{\mathbf{x}}(k+1|k)][\beta(i, k+1|k) - \hat{\mathbf{z}}(k+1|k)]^T,$$

and the innovation covariance is

$$S(k+1) = \sum_{i=1}^{2n_x} \omega_i [\beta(i, k+1|k) - \hat{\mathbf{z}}(k+1|k)][\beta(i, k+1|k) - \hat{\mathbf{z}}(k+1|k)]^T + \sigma_\theta^2.$$

The state and state covariance can then be updated as in the Kalman filter

$$\hat{\mathbf{x}}(k+1|k+1) = \hat{\mathbf{x}}(k+1|k) + W(k+1)\mathbf{v}(k+1)$$

where $\mathbf{v}(k+1) = \mathbf{z}(k+1) - \hat{\mathbf{z}}(k+1|k)$ is the innovation, and

$$P(k+1|k+1) = P(k+1|k) - W(k+1)S(k+1)W^T(k+1).$$

It has been shown that CKF outperforms both the Extended Kalman Filter and the Unscented Kalman Filter (Arasaratnam 2009).

In equation (1), $\mathbf{v}(k)$ is assumed to be a zero mean Gaussian measurement noise. Appropriate values for the covariance or standard deviation need to be determined, taking into account the varying beamwidths and thus potential measurement errors. In order to determine an appropriate measurement noise variance, the array beam patterns from -180 degrees to 180 degrees for 15 degrees increments were plotted and the beamwidths were found. Interpolation was used to calculate beamwidths between the 15 degree increments in bearing. These beamwidths are plotted in red in Figure 8. Also, the measurement error observed for each target bearing for Dataset A is plotted in blue. The *x*-axis represents the actual target bearings from 0 (True North) clockwise to 360^o. It can be seen that a good match to the observed error can be achieved by matching one standard deviation of the bearing measurement error to the beamwidth for the corresponding bearing. Similar results were observed for Dataset B.

The detections from the arrays are processed sequentially to provide state updates at each time step. That is, Array 1 bearing measurements are processed first, and the resulting state estimate is then updated using bear-

ing measurements from Array 2 to obtain the final state estimate for this time step. This process is repeated for the next time instant. Alternatively, one may consider processing bearing measurements from both arrays concurrently.

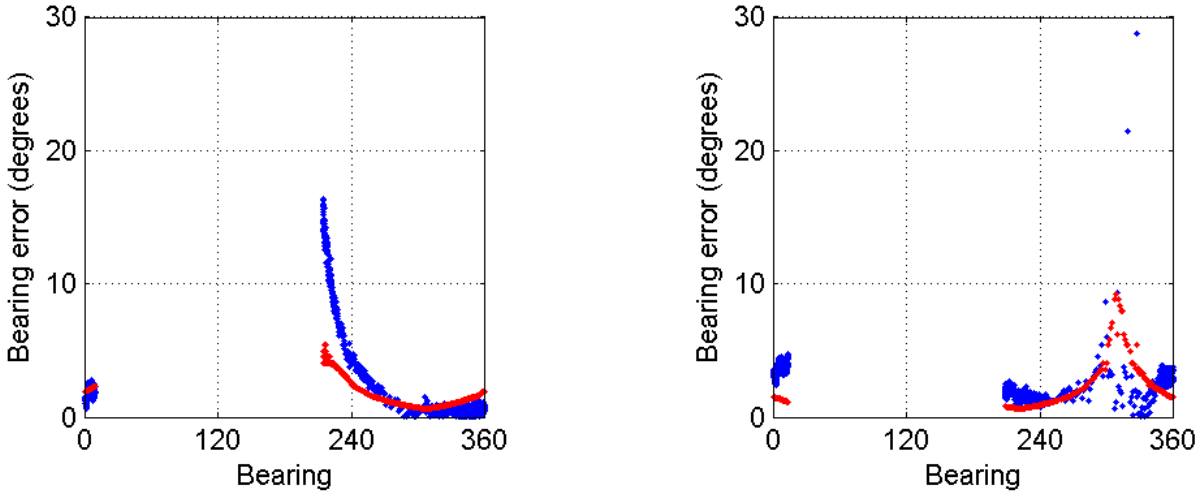

Figure 8 Bearing errors (blue) and 3dB beamwidth for all bearings (red). Array 1 (left) and Array 2 (right)

The presence of false measurements, also known as clutter, is another problem that a tracker must deal with. At a given detection time, a number of measurements may appear near the correct bearing of a track. This requires the tracker to determine how to associate them with the track. *Data Association* is a process within a tracker that decides which measurements to use to update target states using the available detections, including all the false measurements.

We use a multiple target tracking framework and *Global Nearest Neighbour* (GNN) (Blackman and Popoli 1999, Konstantinova, Udvarev and Semerdjiev 2004) data association. For each confirmed track, GNN calculates the normalised distance from each measurement within a validation gate to this track. It then employs the *Munkres algorithm* (Blackman and Popoli 1999, Bondy and Murty 1976) to select a set of measurements such that globally the overall distance of the measurements assigned to tracks from the predicted measurement for that track is minimised. The target states of the confirmed tracks are then updated using the CKF with the assigned global nearest neighbours.

Tentative tracks are initiated for each of the pairwise combinations of bearing measurements from different arrays. A track is initiated at each position in the set. An initiated track is tentative until it passes the *M* out of *N* rule. This rule is satisfied if for at least *M* out of *N* updates, there is at least one measurement within the validation gate of the tentative track.

A track is terminated if one of the following two conditions is satisfied:

Condition 1: estimated track speed exceeds a predetermined maximum target speed,
Condition 2: there is no measurement associated with the track for three consecutive time instants.

The integration time for the seabed array is approximately 8 seconds. We assume that any target of interest, regardless of surface or subsurface contact, is relatively slow moving, and as such, the track initiation is undertaken once for every 10 integration periods using measurements that have not already been associated with an existing track at that time. This reduces the number of tentative tracks that are initiated. It is unlikely to miss the opportunity to initiate a track that follows a target since new tracks are initiated every 80 seconds. If a target is within the detection range of an array, it is very unlikely for it to travel outside this detection range within this short period of time.

4 TARGET TRACKING RESULTS

The CKF with GNN data association described in Section 3 is selected to track the target using measured bearings. The tracking result for Dataset A using the experimentally obtained bearing measurements is shown in

Figure 9 (left) and the associated position errors are shown in the same figure (right). The true trajectory of the merchant ship Target A is shown in green. The estimated tracks from the tracker are shown in black. There is one false track resulting from the ambiguous bearing detections from the linear arrays. The target-associated track generally follows the target. However, it starts at a fair distance away from the true starting position of the target. This is caused by the near 16 degrees bearing measurement bias at the beginning of the scenario. The track also has a loop as observed in the true target trajectory. While the target travels towards north, the ratio between the range of the target from the arrays and the distance between the two arrays grows. The position error grows larger as this ratio grows. This is why the track error grows as the target moves away from the arrays. We may refer to this as the *range*-to-*baseline ratio problem*. Mathematically, the transformation of detections in bearing space into locations in the *xy* plane is highly nonlinear. A small error in bearings may cause large error in location and velocity in Cartesian coordinates as seen in both data sets. This is particularly true of targets at long range from the arrays, where even a small bearing error can result in large positional error.

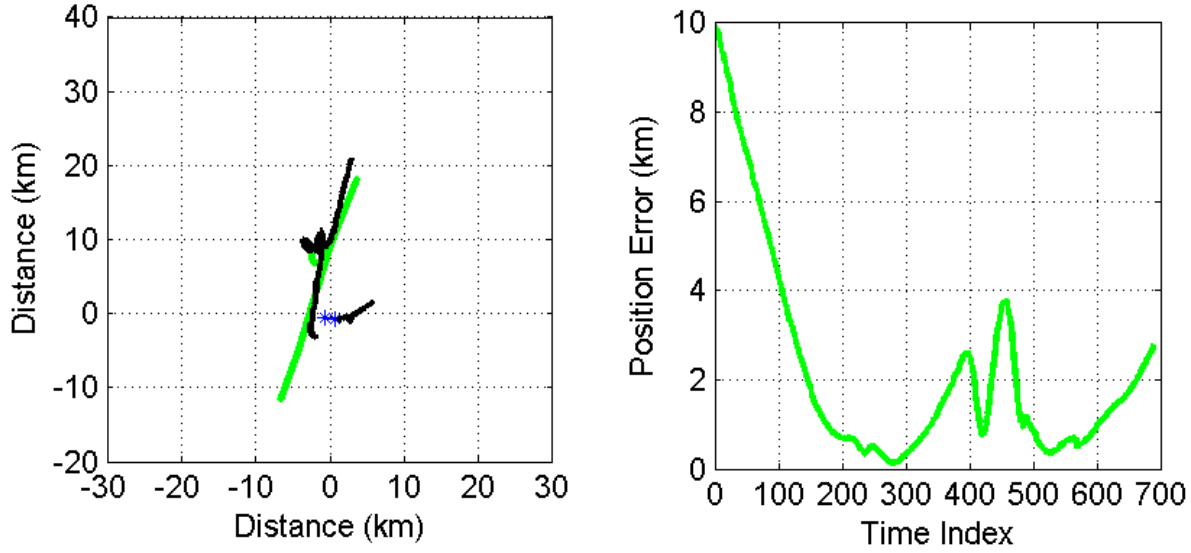

Figure 9 Tracking result for Dataset A (left) and the position errors (right)

For Dataset B, the tracking algorithm is tested on data during the time period 00:25 to 00:45. The reason is to initiate the tracks automatically within reasonable vicinity of the true target locations and to avoid the region of bearing measurement bias. The tracking result and the associated position errors are shown in Figure 10. The false tracks are caused by the false bearing detections from the left/right ambiguity associated with a line array. The tracker performs well on this dataset, demonstrating an ability to track both targets.

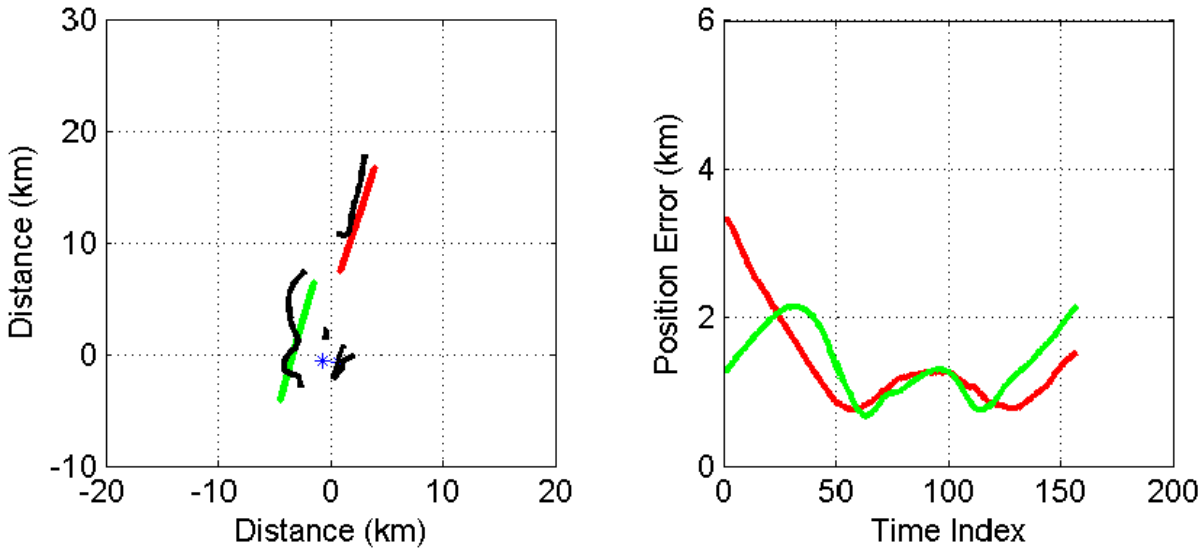

Figure 10 Tracking results for Dataset B during the time period 00:25 and 00:45 (left) and the position errors for red and green targets (right)

5 CONCLUSIONS

Target tracking using seabed array bearing detections is investigated in this paper. Multitarget tracking using bearing detections from two or more arrays can perform well as long as a severe range-to-baseline ratio problem is not present. That is the ratio of the distance between the target and the centroid of the arrays and the distance between arrays is not large. It is found that the range-to-baseline ratio problem is a major challenge for bearings only tracking using seabed arrays. The range-to-baseline ratio problem is a reflection of the fact that the transformation of bearing detections from multiple arrays in bearing space to target location in *xy* space is highly nonlinear. Small errors in bearings may result in very large error in target location and velocity estimates. This problem will limit the robustness of an automatic bearing only target tracker for seabed arrays. Attempts to mitigate the range-to-baseline ratio problem by increasing the separation between arrays will, in practice, be unlikely to work either. If the arrays are deployed far apart, it is very unlikely to have simultaneous pressure detections on multiple arrays.

Another challenge observed for tracking using experimental seabed array data was that of quantised measurements. The beamformer used to process the array data used one degree increments between consecutive beams, resulting in discrete bearing measurements. Typical measurement models used in trackers assume continuous valued measurement models and this model mismatch impacts the performance of the tracker. Alternative measurement models that account for the quantised measurements may give improved tracking performance.

Finally, the experimental bearing data was shown to have varying bias, particularly observed near end-fire of the arrays. Unless explicitly included in the measurement model, bearing measurement biases inherently result in a position error in the tracker. Further investigation of a model for the bias or online estimation of the bias within the tracker may result in improved tracking performance.

REFERENCES

Arasaratnam,I. 2009. *Cubature Kalman filtering: theory & applications,* Ph.D thesis, McMaster Univeristy.
Arasaratnam,I. and Haykin, S. 2009. “Cubature Kalman filters”, *IEEE Transactions on Automatic Control,* 54(6), 1254-1269.
Arasaratnam,I., Haykin, S. and Hurd, T. 2010. “Cubature Kalman filtering for continuous-discrete system: theory and simulations”, *IEEE Transactions on Signal Processing,* 58(10), 4977-4993.
Bar-Shalom, Y. and Fortmann, T. 1988. *Tracking and data association*, Academic Press.
Blackman, B. and Popoli, R. 1999. *Design and analysis of modern tracking systems*, Artech House.
Bondy , J. and Murty, U. 1976. *Graph theory with applications*, Elsevier Science Ltd/North-Holland.
Konstantinova ,P., Udvarev, A. and Semerdjiev, T. 2003, “A study of a target tracking algorithm using global nearest neighbour approach”*, Proceedings of the 4th international conference on computer systems and technologies, 290-295.*
Ristic, B., Arulampalam, S., and Gordon, N. 2004. *Beyond Kalman filtering: particle filters for tracking applications*”, Artech House.